Characterization of the Substrate Mimic Bound to Engineered Prostacyclin Synthase in Solution Using High-Resolution NMR Spectroscopy and Mutagenesis: Implication of the Molecular Mechanism in Biosynthesis of Prostacyclin†

Ke-He Ruan,* Jiaxin Wu, and Vanessa Cervantes

The Center for Experimental Therapeutics and PharmacoInformatics and Department of Pharmacological and Pharmaceutical Sciences, College of Pharmacy, University of Houston, Houston, Texas 77204

Received August 17, 2007; Revised Manuscript Received October 19, 2007

ABSTRACT: High-resolution NMR spectroscopy was used to determine the docking of a substrate (prostaglandin H_2) mimic (U46619) to the engineered prostacyclin (PGI_2) synthase (PGIS) in solution. The binding of U46619 to the PGIS protein was demonstrated by 1D NMR titration, and the significant perturbation of the chemical shifts of protons at C-11, H2C, and H20 of U46619 were observed upon U46619 binding to the engineered PGIS in a concentration-dependent manner. The detailed conformational change and 3D structure of the PGIS-bound U46619 were further demonstrated by 2D ^{1}H NMR experiments using the transferred NOE technique. The distances between the protons H20 and H2, H18 and H2, and H18 and H4 are shorter following their binding to the PGIS in solution—down to within 5 Å. These shorter distances resulted in a widely open conformation, where the triangle shape of the unbound U46619 changed to a more compact conformation with an oval shape. The bound conformation of U46619 fits the crystal structure of the PGIS substrate binding pocket considerably better than that of the unbound U46619. The residues important to the substrate binding in the active site pocket of PGIS were also predicted. For example, Trp282 could be one of the most important residues and is suspected to play a role in the determination of specific catalytic function, which has been established by the docking studies using the NMR structure of the PGIS-bound form of U46619 and the PGIS crystal structure. These studies have provided the structural information for the interaction of the PGIS with its substrate mimic. The noted conformational changes where the C-6 position is closer to the C-9 position of U46619 provided the first experimental data for understanding the molecular mechanism of the catalytic function of PGIS in the isomerization of PGH_2 to prostacyclin.

The biosynthesis of the different prostanoids involves the conversion of arachidonic acid (AA)[1] to the unstable prostaglandin H_2 (PGH_2; Figure 1) by cyclooxygenase (COX) isoform-1 (COX-1) or -2 (COX-2) and then the isomerization of PGH_2 to the biologically active prostaglandins (PGs) E_2 (PGE_2), PGD_2, PGF_2, and PGI_2 and thromboxane A_2 (TXA_2) by their corresponding COX-downstream synthases (*1*−*10*). The synthesized prostanoids mediate diverse and opposite pathophysiological processes within the vascular, nervous, reproductive, and other systems as well as cancers. For example, TXA_2, synthesized by TXA_2 synthase (TXAS), has been implicated as a proaggregatory and vasoconstricting mediator in various pathophysiological conditions such as stroke and heart diseases (*7*, *8*). In contrast, PGI_2 synthesized from PGI_2 synthase reveals opposing characteristics when compared to TXA_2. Little structural information is available for the molecular basis of the prostanoid biosynthesis mediated by the COX-downstream synthases. This becomes a major obstacle for further understanding the molecular mechanisms of their specific catalytic functions. In the past, some attempts have been made to understand the molecular

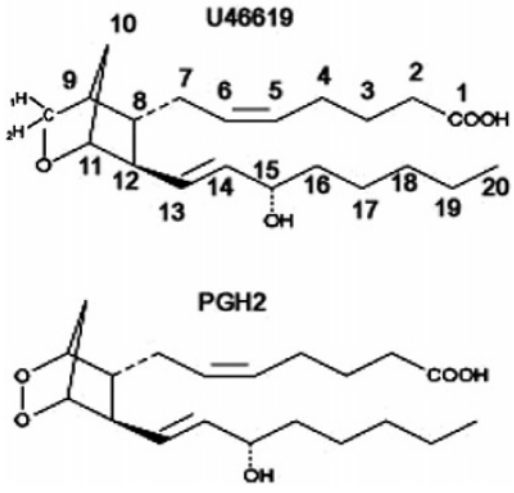

FIGURE 1: Chemical structure of U46619 and PGH_2.

† This work was supported by NIH Grants HL56712 and HL79389.

* To whom correspondence should be addressed. Phone: (713) 743-1771. Fax: (713) 743-1884. E-mail: khruan@uh.edu.

[1] Abbreviations: AA, arachidonic acid; PGI_2, prostacyclin or prostaglandin I_2; TXAS, thromboxane A_2 synthase; PGIS, PGI_2 or prostacyclin synthase; PGH_2, prostaglandin H_2; ER, endoplasmic reticulum; NMR, nuclear magnetic resonance; DQF-COSY, double-quantum-filtered correlation spectroscopy; NOE, nuclear Overhauser effect; NOESY, nuclear Overhauser effect spectroscopy; TOCSY, total correlation spectroscopy; 1D, one dimensional; 2D, two dimensional; 3D, three dimensional; DSS, 2,2-dimethyl-2-silapentane-5-sulfonic acid, NMR calibration standard.

10.1021/bi701671q CCC: $40.75
Published on Web 12/15/2007

mechanism behind the different substrate recognition and binding sites that adopt the different conformations of PGH_2 for PGIS and TXAS. Different orientations of PGH_2 in the active site pockets of TXAS and PGI_2 synthase (PGIS), with respect to the heme iron position, have been proposed by Hecker and Ullrich (*11*). Their spectroscopic studies, which involve the stable PGH_2 analogues U44069 and U46619 (Figure 1) with a modification of the *endo*-peroxide oxygen atom at the C-9 or C-11 position of PGH_2, have suggested that the C-9 *endo*-peroxide oxygen of PGH_2 is likely to interact with the heme ferric iron of the TXAS molecule. In contrast, the C-11 *endo*-peroxide oxygen of PGH_2 interacts with the heme ferric iron of PGIS. The current spectroscopic studies, which involve the use of different ligands to probe the substrate binding pockets, have indicated that PGIS has a much narrower substrate binding pocket than TXAS (*12*). These spectroscopic assays provided an important insight, suggesting that PGH_2 adopts different conformations while in the substrate binding sites of the COX-downstream synthases. The very recent crystal structure of the engineered PGIS has confirmed the earlier observation, in which the substrate binding pocket of PGIS is relatively smaller than that of other P450's (*13*). In addition, the binding of the PGH_2 mimic U44069 to the engineered TXAS in solution has been recently characterized by our laboratory using high-resolution NMR spectroscopic studies (*14*). The studies successfully revealed that the PGH_2 mimic underwent a conformational change when bound to the active TXAS protein in solution. This conformational change was favorable to the ligand docking into the pocket of the enzyme's substrate binding site. This bound form conformation of the ligand should facilitate an illustration of the substrate pocket. However, the lack of a crystal structure for TXAS has created a challenge for further identifying the exact residues of the synthase which are involved in the ligand docking, but since the crystal structure of PGIS has been solved, we were able to overcome this limitation for PGIS and further identify the molecular mechanisms for the catalytic function of the synthase using the solution structure of the substrate mimic. In this paper we describe the first studies to characterize the binding of the substrate mimic and PGIS in solution using high-resolution NMR spectroscopy, reveal the molecular basis of its catalytic function in the isomerization of PGH_2 to PGI_2, and attempt to find the possible key residues involved in the determination of the specific catalytic function. The residue Trp282 (nonconserved in TXAS) was predicted as one of the key residues that might be involved in the specific catalytic activity of PGIS. All of the studies were carried out by docking of the NMR structure ligand to the crystal structure of the PGIS protein.

EXPERIMENTAL PROCEDURES

Materials. D_2O and ethanol-d_6 were purchased from Cambridge Isotope Laboratories (Andover, MA). U46619 (Figure 1), a stable analogue of PGH_2, was obtained from Cayman Chemical (Ann Arbor, MI). All other chemicals were purchased from Sigma.

Preparation of Engineered Soluble PGIS. The protein of the engineered soluble PGIS was a gift from Dr. Lee-Ho Wang's laboratory (University of Texas Health Science Center, Houston, TX). The details for the preparation of the engineered soluble PGIS have previously been published (*15*). Briefly, a soluble form of PGIS was generated by replacing the N-terminal membrane-anchoring domain of PGIS with the N-terminal sequence P4502C5 MAKKTSS and a four-histidine tag at the carboxyl terminus to facilitate purification. The resultant chimeric protein [2C5/Δ(1−17)-PGIS, referred to as "PGIS" below] was expressed in bacteria as a cytosolic and monomeric protein that could yield approximately 8 mg of soluble PGIS/L of bacterial culture, with a purity of more than 95% by electrophoresis (*15*).

NMR Experiments. For the NMR experiment of the free form ligand, U46619 (final concentration of 5.2 mM) was dissolved in 0.55 mL of 20 mM sodium phosphate buffer, pH 7.5, containing 10% ethanol-d_6 and D_2O (to provide a lock signal) and then used for determination of the 1D and 2D (DQF-COSY, TOCSY, and NOESY) ^1H spectra. For the NMR titration experiment, soluble PGIS was dissolved in 0.5 mL of sodium phosphate buffer, pH 7.5, containing 150 mM NaCl and 10% D_2O and the 1D ^1H spectra for PGIS were acquired. Later, different amounts (5, 10, 20, and 50 μL) of U46619 in ethanol-d_6 were added to the sample (1 mg/50 μL) and incubated at 298 K for 20 min, and the 1D spectra were acquired again. The 2D DQF-COSY, TOCSY, and NOESY spectra for the final mixture of the titration (4.8 mM U46619 and 80 μM PGIS, in 0.55 mL of 20 mM sodium phosphate, pH 7.5, containing 9% ethanol-d_6 and 9% D_2O) were then recorded. All NMR experiments were carried out on a Bruker Avance 600 MHz NMR spectrometer with a 5 mm triple-resonance probe at 298 K. The water peak was suppressed by the excitation sculpting method (*16*). All 1D spectra contain 16K data points. NOESY and TOCSY spectra contain 2048 × 512 data points, and the DQF-COSY spectra contain 4096 × 512 data points. The NOESY spectra were recorded with a mixing time of 150 and 300 ms. The TOCSY spectra were carried out with an MLEV-17 spin-lock pulse sequence with a total mixing time of 70 ms. Quadrature detection was achieved in F1 by the states-TPPI method. The NMR data were processed using the Felix 2000 program (Accelrys, San Diego, CA). Shifted sine-bell window functions of 0° (for DQF-COSY), 60° (for TOCSY), or 90° (for NOESY) were used in both dimensions. Chemical shifts were referenced to the internal standard DSS (contained in D_2O), which was set to 0 ppm.

Calculation of Structures and Docking of U46619 into the PGIS Active Site. The overall conformation of the free U46619 or the PGIS-bound U46619 was determined through the inter-proton distances derived from the NOESY cross-peaks using a distance bound method (*17*). The NOE cross-peaks were first assigned, and the volumes were measured and converted into upper bounds of the inter-proton distance constraints using the Felix 2000 program. The strong, medium, and weak peaks were set to correspond to upper bound distances of 2.7, 3.5, and 5.0 Å, respectively. Distance constraints were input manually into the Discover program within the Insight II package (Accelrys), and restrained energy minimizations consisting of 1000 steps of conjugate gradient algorithm were then carried out to generate the structure of U46619. For the docking studies of U46619, the PDB file of the PGIS (PDB ID 2IAG) was converted into a file with hydrogen atoms using the Biopolymer module of the Insight II program. U46619 was docked into the substrate binding site of the crystal structure of PGIS with the initial configuration, where the O-11 atom of U46619 is

directed toward the ferric iron on the heme on the basis of the previous paper (*11*). The energy minimization using the Discover program with 1000 steps of steepest descent algorithm was used to optimize the docking. The force field used was the consistent value force field (CVFF) with modified nonbond parameters for the heme (*18*, *19*).

RESULTS

PGIS Substrate Mimic U46619. Two synthetic molecules, U44069 (not shown) and U46619 (Figure 1), are widely used as PGH_2 mimics to study the binding of COX-downstream synthases with their substrate. Both molecules have a chemical structure identical to that of PGH_2 (Figure 1), with the exception of the replacement of the C-11 (for U44069, data not shown) or C-9 (for U46619, Figure 1) *endo*-peroxide by a carbon (*17*). With the single-atom modification, U44069 and U46619 became highly stable in comparison to PGH_2, which had a half-life of only a few minutes in solution. The binding affinity of U46619 for PGIS is much higher than for TXAS. In contrast, U44069 has a higher binding affinity for TXAS than for PGIS (*11*). Therefore, U46619 is a very useful analogue to probe the conformation of PGH_2 bound to PGIS.

Preparation of the Engineered Soluble Human PGIS. The engineered human PGIS, containing an alternation of the N-terminal membrane domain, was prepared as described (*15*). After purification, the binding activity of the engineered PGIS to its substrate analogue, U46619, was characterized using absorption spectroscopy and MCD (magnetic circular dichroism) methods (*15*). The binding activity of soluble, engineered PGIS to U46619 had a K_d of 36 μM, which is close to that of the wild-type PGIS (30 μM; *15*).

Binding of the Substrate Analogue U46619 to the Engineered PGIS Characterized by 1D ^{1}H NMR Titration Experiments. In previous NMR structural studies for the interaction of U44069 with TXAS, we have found that the binding of U44069 to TXAS causes a conformational change in which an open hairpin structure is converted to a more compact oval-like structure (*14*). This was the first experimental evidence to show the docking of PGH_2 to one of the COX-downstream synthases in solution and imply that PGH_2, when catalyzed by different COX-downstream synthases, needs the correct conformation to fit the different active sites of the synthases. It could be a key factor in determining the specificities of the synthases' catalytic functions in their biosynthesis of the different prostanoids. PGIS is similar to TXAS because they both belong to the microsomal P450's and share significant homologies in their backbone structures and substrate binding sites (*20*). To see the docking of the PGH_2 to PGIS, 1D ^{1}H NMR titration experiments were performed to determine the binding of U46619 to PGIS in solution, as described in the Experimental Procedures. Upon binding of U46619 to the PGIS, the chemical shifts of the proton resonance signals of both the ligand and protein were affected. Since PGIS has a molecular mass of about 60 kDa and its NMR signal is difficult to observe, we focus primarily on the changes of the chemical shifts of U44069. Thus, the 1D ^{1}H NMR titration experiments were designed to perform the experiment in the presence of a large amount of U46619 and a very small amount of PGIS protein to exclude the signals of the protein. The molar ratios of U46619 to PGIS in experiments B, C, D, and E in Figure 2 were 57:1, 28.5:1, 14.3:1, and 5.7:1, respectively. Significant perturbations of the proton chemical shifts at H11, H2C, and H20 of U46619 were observed following the addition of the engineered PGIS in a concentration-dependent manner during the titration experiments (Figures 2 and 3).

In contrast, shifts of the other U46619 protons (such as H12) were not significantly changed. These results provide evidence that U46619 was showing some interaction upon binding to PGIS in solution and the U44069 protons H11, H2C, and H20 were likely involved in the direct and/or indirect contact with the active site residues of the PGIS protein.

Detection and Characterization of the Substrate Analogue U46619 Binding to the Engineered PGIS by the Transferred NOE Effect. The exchange-transferred nuclear Overhauser effect NMR spectroscopy (transferred NOE, trNOE, or etNOE) has proven to be a useful technique for studying the bound conformation of flexible ligands and to screen mixtures of small molecules for binding activity.

When the free state and bound state of a ligand undergo a fast exchange (normally requires $K_d > 1$ μM), the NMR signal will be a single peak at the weighted-average position over the free and bound signals. The free-state ligand is a small molecule with a fast tumbling rate, which shows a weak positive NOE that may build up slowly. Conversely, the bound state of the ligand has a slow tumbling rate and large negative NOEs that quickly build up, due to the large molecular weight of the ligand−protein complex (*21*, *22*). In trNOE experiments, the NOESY spectrum of the ligand is recorded in the presence of a very small amount of proteins. The cross-peak intensities of the NOESY spectrum could be predominantly determined by the bound-state NOEs. Therefore, by measuring the intensities of the NOE cross-peaks, the inter-proton distances in the bound state can be estimated and used to calculate the bound-state conformation. Also, the ligand binding to the protein may be indicated by a change in the sign of NOE cross-peaks from negative (free ligand, positive NOE) to positive (bound ligand, negative NOE).

In these studies, 2D ^{1}H NMR spectra, NOESY, DQF-COSY, and TOCSY, for U46619, in the presence and absence of the engineered soluble PGIS, were recorded using 150 and 300 ms mixing times. For the 2D experiments, the ratio of U46619 to PGIS protein was approximately 57:1, which gave a strong signal for the U46619 and little interference from the broad and weak protein peaks. The proton resonance assignments for U46619 alone were accomplished on the basis of the proton chemical shifts and the through-bond coupling detected by DQF-COSY and TOCSY. Figure 4 shows an example of the 2D NMR assignments for the U46619 2D spectra recorded using 300 ms mixing time.

The resonance assignments of U46619 in the presence of PGIS were obtained by comparing the spectra of the mixture with that of the free U46619. The binding of U46619 to the engineered soluble PGIS protein was clearly established by the identification of two major changes in the NOESY spectra: (a) The intramolecular NOE cross-peaks of U46619 changed from the negative phase (Figure 5, top panel, small molecule showing a negative phase) to the positive phase (Figure 5, middle panel; U44069 bound to the active PGIS

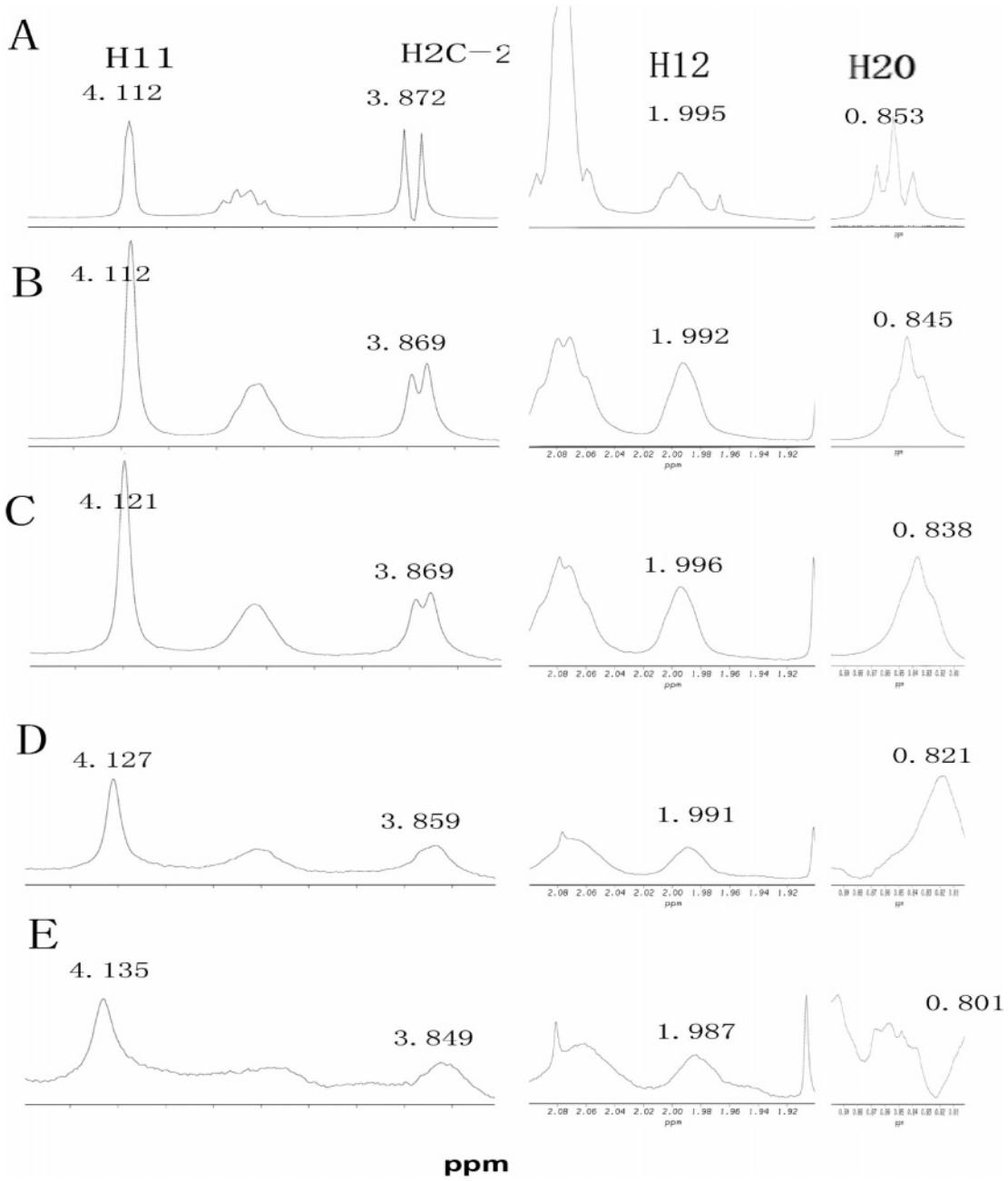

FIGURE 2: 1D NMR titration of U46619 bound to the engineered PGIS. Free unbound U46619 is shown (A). The chemical shift signals of U46619 were perturbed by the addition of PGIS protein at ratios of 57:1 (B), 28.5:1 (C), 14.3:1 (D), and 5.7:1 (E).

became a large complex with a positive phase). In contrast, a nonphase change was observed in the presence of the inactive PGIS protein (Figure 5, bottom panel). (b) New NOE cross-peaks were observed in the NOESY spectrum of U46619 with the active PGIS protein (Figure 6), which accounted for the ligand's interaction with PGIS. For example, the NOE cross-peaks of H20/H2, H18/H2, and H18/H4, identified in the NOESY spectrum of U46619 with the engineered PGIS (Figure 6B), were not found in the NOESY spectrum of the free U46619 (Figure 6A). This indicates that the distances between H20 and H2, H18 and H2, and H18 and H4 are closer upon binding to the PGIS, down to within 5 Å.

3D Solution Structure of the PGIS-Bound U46619. The complete assignments for the proton resonances of U46619 in the presence of the engineered PGIS allowed us to generate 32 NOE (for a 300 ms mixing time) constraints from the NOESY spectrum (Table 1). The similar 31 NOE constraints were also obtained with a 150 ms mixing time (data not shown). Two refined 3D structures of the PGIS-bound U46619 were obtained by structural calculations using the experimental distance constraints (150 and 300 ms mixing times, Figure 7A). The solution NMR structure of the free U46619 (Figure 7B) was also generated by a similar approach. To show the differences between the structures of U46619 in the free and bound forms in solution, the free form structure was superimposed with one of the bound form structures (Figure 7C). It should also be indicated that all of the structures generated from their NOE constraints were satisfied by calculating the input restraints' satisfaction using the Insight II program. In the free form of U46619, the two arms (α and ω chains) were widely open with a distance of approximately 8.9 Å. In contrast, the PGIS-bound form of U46619 adopted a compact conformation with an oval shape,

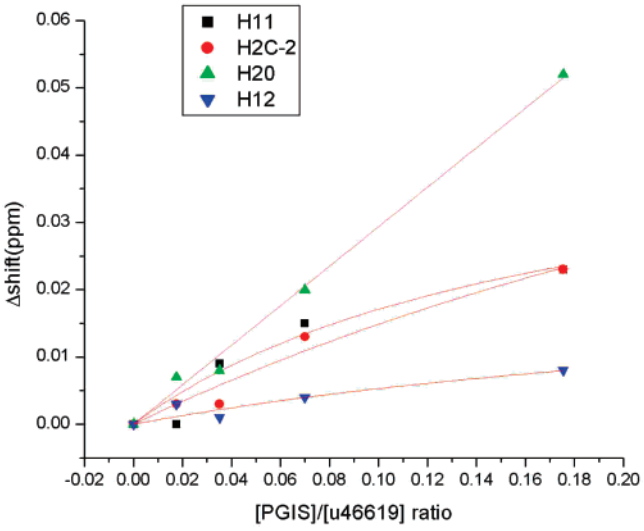

FIGURE 3: Perturbations of the proton chemical shifts of U46619 in the presence of the engineered PGIS protein. The altered chemical shifts of H11, H2C, and H20 resulting from the addition of the engineered PGIS are plotted. The unchanged chemical shift of H12 was also plotted as an internal control.

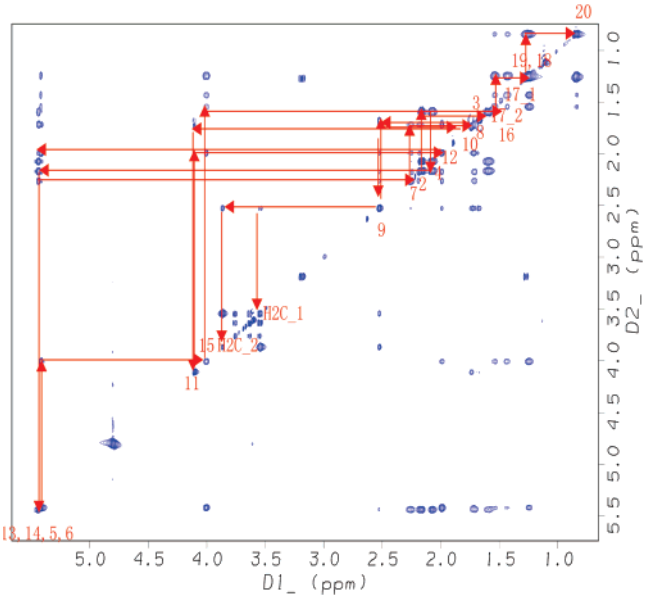

FIGURE 4: TOCSY spectrum showing the resonance assignments of the free U46619 in solution. The coupling network between protons on adjacent carbons is indicated.

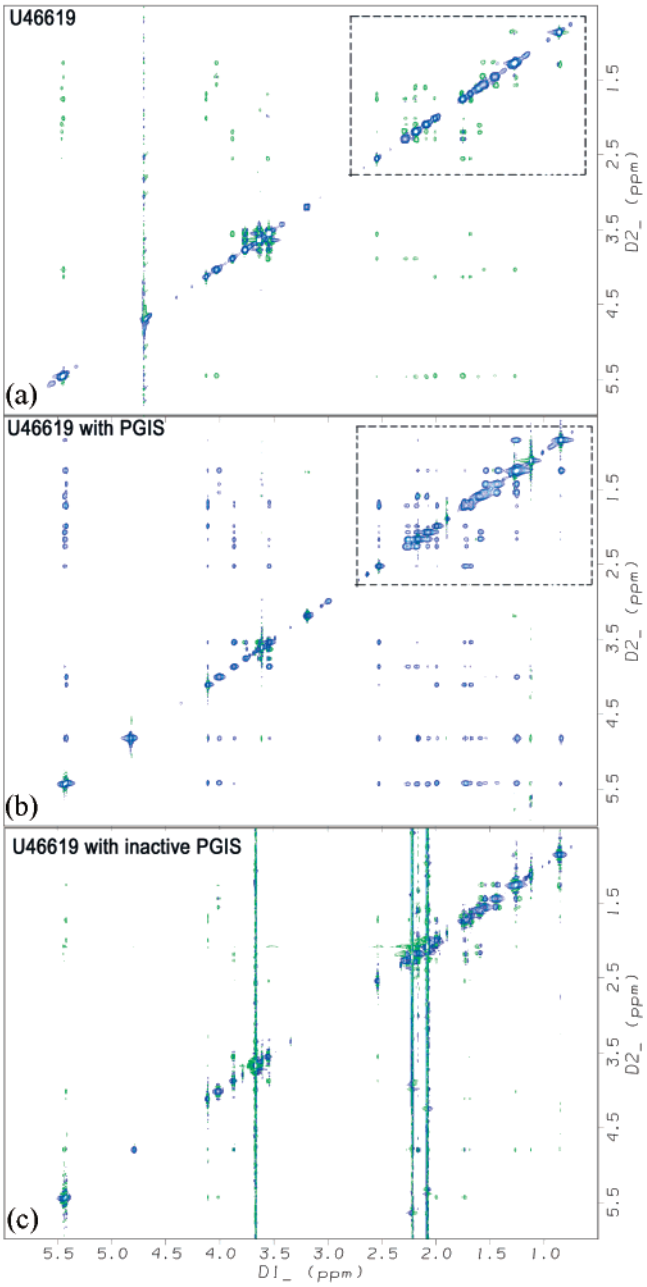

FIGURE 5: Contour plots of the NOESY spectra (300 ms mixing time) of U46619 alone (top panel) and with the active (middle panel) or inactive (bottom panel) PGIS protein. The cross-peaks in (A) and (C) are negative (green color), corresponding to the positive NOEs, whereas in (B) some of the cross-peaks are positive (blue color), indicating the negative NOEs. The detailed cross-peaks inside the dashed line frames in the top and middle panels are shown in Figure 6.

in which the two arms became closer, generating a distance of approximately 5.3 Å (Figure 7C). This distance change between the α and *ω* chains is similar to that of the U44069 bound to TXAS. However, some differences can be observed in the ring region.

Docking of the PGIS-Bound U46619 Conformation with the Substrate Binding Pocket of the Crystal Structure of the Engineered Human PGIS. The crystal structure of the engineered human PGIS was solved very recently and showed that the PGIS active site is relatively small compared with that of other P450's. The docking module of Insight II was used to monitor the intermolecular energy between U46619 and PGIS (with a cutoff value of 20 Å). Docking of the NMR- determined structure of the free form of PGH_2 (with the α and *ω* chains widely open) into the active site of the PGIS crystal structure caused severe steric clashes resulting from the unreasonable energy increase of the overlapping atoms between the ligand and the side chains of the protein. This information implies that conformational changes are necessary when the substrate binds to PGIS, which is consistent with our NMR experimental observation in the determination of the bound form structure of U46619 (Figure 7). We then docked the well-defined conformation of the bound form of U46619 into the PGIS active site to see whether there was a better fit than that of the free form U46619. The docking was carried out by the following strategies: (a) The substrate binding site of PGIS was identified by the crystal structure presentation (*13*). (b) The

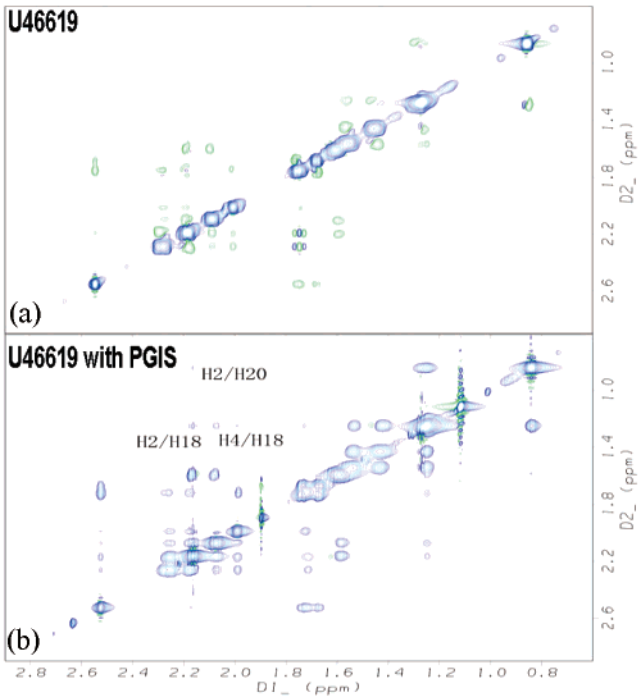

FIGURE 6: Intramolecular NOEs of U44069 bound to the engineered PGIS protein. The new intramolecular NOEs of U46619 appeared after interaction with active PGIS (B) in comparison with its free state (A). The new NOE cross-peaks were labeled with the corresponding resonance assignments in the first and second dimensions.

Table 1: NOE Constraints of the Bound Form of U46619 Used To Generate the 3D Conformation

proton pair	distance (Å)	proton pair	distance (Å)
H14/H18	5.0	H7-1/H2C-2	3.5
H13/H18	2.7	H7-2/H2C-2	3.5
H13/H12	3.5	H9/H2C-1	2.7
H14/H12	3.5	H12/H8	2.7
H5/H4	2.7	H20/H19	2.7
H7-2/H6	3.5	H2C-1/H10a	2.7
H9/H6	5.0	H2C-1/H10b	5.0
H14/H15	3.5	H9/H10a	5.0
H13/H15	3.5	H9/H10b	3.5
H14/H11	5.0	H9/H8	3.5
H13/H11	5.0	H4/H3	2.7
H15/H18	5.0	H2/H3	2.7
H11/H10a	5.0	H18/H17	2.7
H11/H10b	5.0	H18/H16-2	2.7
H12/H11	3.5	H18/H16-1	2.7
H2C-2/H12	5.0	H20/H2	5.0

O-11 atom of the PGIS-bound form of U46619 was set in the position in contact with the heme ferric iron on the basis of the earlier spectroscopic analyses (*11*). (c) The overall contact of U46619 with the residues of the substrate binding followed our earlier mutagenesis studies (*23*). For example, the Leu214 and Pro215 residues in the F/G loop, which are known to be important residues involved in the substrate binding (*23*), were set near the ends of the α and *ω* chains of U46619. (d) By fixing the positions of the head and the end of U46619 in the pocket, the best fit of the U46619/PGIS docking was obtained. (e) By using the Insight II docking module, a position for U46619 with the lowest intermolecular energy was determined. (f) Finally, the entire U46619/PGIS complex was subject to energy minimization using the Discover program for further refinement, with fixed

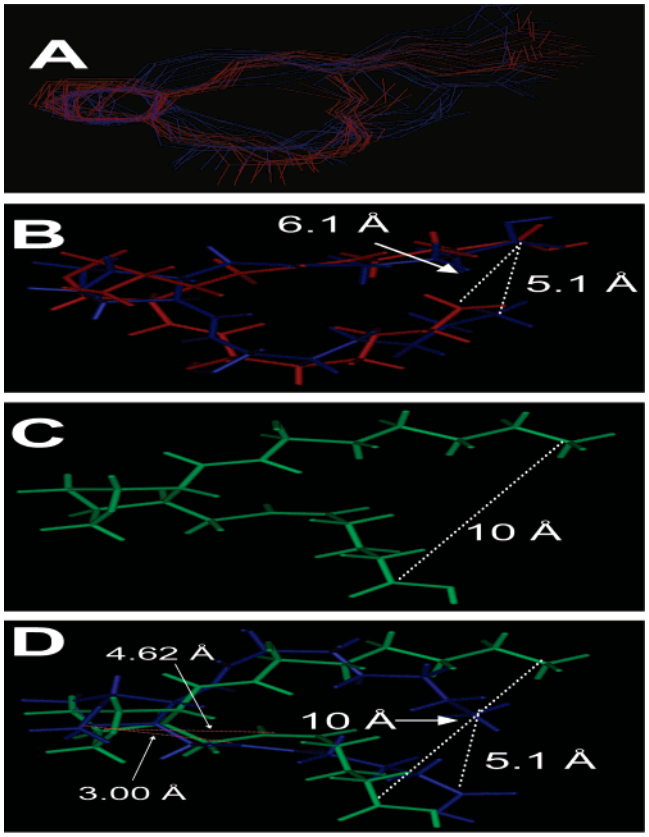

FIGURE 7: NMR structures of U46619. (A) The structures of the PGIS-bound form of U46619 generated from trNOE experiments using 150 ms (red color (10 structures)) and 300 ms (blue color (10 structures)) mixing times were superimposed. (B) Two of the final averaged structures of the PGIS-bound U46619 generated with 150 ms (red color) and 300 ms (blue color) mixing times were superimposed. (C) Free form of the NMR structure of U46619. (D) Superimposed free form (green color) and bound from (blue color, 300 ms) of U46619. The superimposed image (D) shows the distances between C-6 and C-9 (red dotted lines) and between the α and *β* carbons (white dotted lines) of U46619.

constraints applied to the all α carbons of PGIS and all the heavy atoms of the heme molecule. Also, weak distance constraints of the upper limit (4 Å) were applied to the distance between the ferric iron and the O-11 atom of U46619. The conformation of U46619, after the complex energy minimization, had little difference when compared with the original bound conformation calculated from the NMR data. The intermolecular energy was −45 (kcal/mol)/Å, which indicated that the binding of U46619 to PGIS causes a decrease in intermolecular energy. This docking has further improved the NMR structure of the bound form of U46619 calculated from the semiqualitative NOE data and proven that the bound conformation of U46619 actually fits the PGIS substrate pocket (Figure 8). Some key residues which are likely to be involved in the substrate binding, such as Y99, L103, W282, and F483, are also highlighted in Figure 8.

Docking Analysis of the Key Residue Trp282 in the Substrate Binding Pocket Interacting with U46619. To test whether the residues in contact with U46619 in the PGIS substrate binding pocket (identified by the previous docking studies) are involved in the regulation of the enzyme catalytic function, a computational approach was used to replace the Trp282 residue (one of the key residues listed in the above

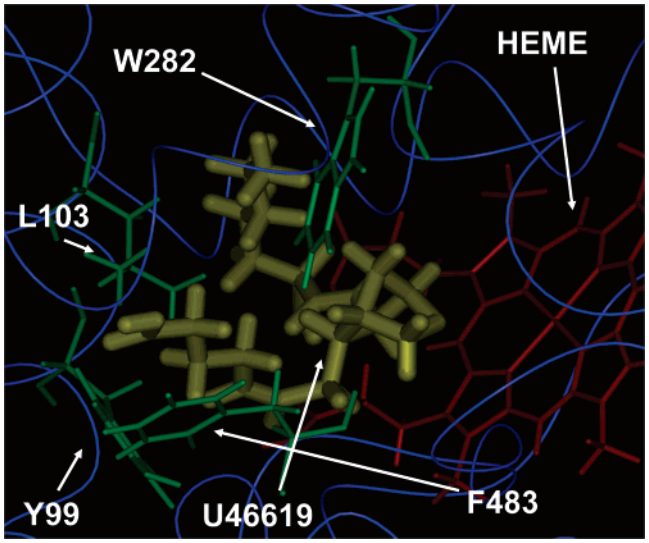

FIGURE 8: Docking of U46619 into the putative substrate binding pocket of the PGIS crystal structure. The molecules displayed are heme (red), U46619 (yellow), the PGIS protein sequence (blue lines), and the side chain of W282 (green). Other residues likely involved in the ligand interaction are also labeled.

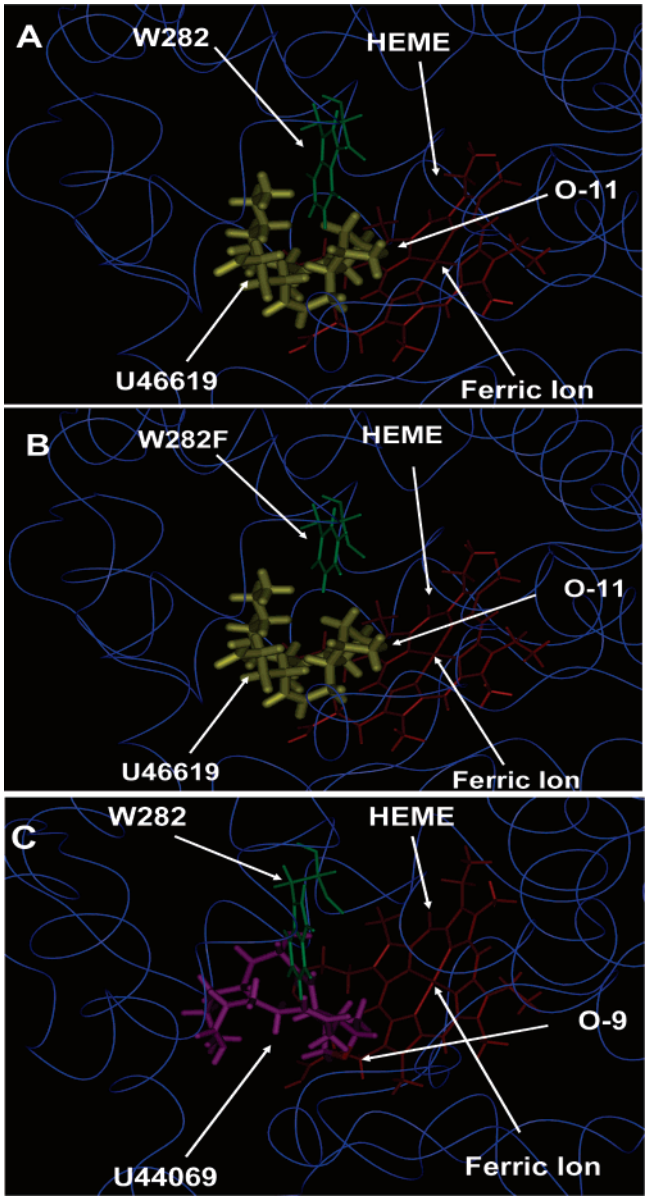

FIGURE 9: In silico mutation for PGIS Trp282 and the comparison of the PGIS-bound form of U46619 and TXAS-bound form of U44069 (*14*) docked into the active site of the PGIS crystal structure. Bound form of the NMR structure of U46619 docked into the active site of the wild type (A) or W282F mutant (B) of PGIS. The TXAS-bound form of the NMR structure of U44069 replaced by the PGIS-bound form of U46619 in the active site shown in panel A is also displayed (C).

section) with a Phe residue (W282F), which has a similarly sized side chain. Figure 9A shows that the W282 side chain is very likely to play a role in constraining the docking orientation of U46619 when it moves into the 3D pocket of wild-type PGIS. In this case, U46619 can only have a "fixed" orientation when accessing the active site. This could be a factor in arranging the C-11 *endo*-peroxide of PGH_2 to contact the heme iron for the specific isomerization of the substrate to PGI_2 (Figure 9A). However, in the W282F mutant, the F282 residue in the binding pocket shows a loose contact and perhaps lost the constraints with U46619, which led to the U46619 binding to the pocket in an "unfixed" orientation (Figure 9B). The conformation of the TXAS-bound U44069 was superimposed with the PGIS-bound U46619 in the active site pocket of PGIS (Figure 9C). Although the PGIS-bound U46619 fit into the pocket perfectly, the TXAS-bound U44069 could not fit the pocket as well due to several impairments. The side chain conformation of U44069 (Figure 9C) would not fit the Trp282 configuration as did the U46619 side chain (Figure 9A). The *endo*-peroxide at the C9 position of U44069 was out of place and contacting the Fe^{2+} atom of the heme. These results further suggested that the Trp282 configuration (with the bound form of U46619 observed in the NMR structure) is involved in the control of the specificity and affinity of the substrate−enzyme docking in PGIS.

DISCUSSION

Typically, the studies involving substrate binding to enzymes are simply monitored by observing changes in the products or substrates using spectroscopic and other assay methods. These methods are relatively simple and useful for the basic characterization of the enzyme activities. However, they cannot provide detailed structural information regarding the substrate's actual binding to the enzymes. Cocrystallization of the substrate analogues with the enzymes has been the classic method used to study the enzyme catalytic mechanisms from a structural point of view. However, it is time-consuming in getting the complex crystal, data collection, and interpretation. NMR spectroscopic techniques, such as trNOE, saturation transferred difference (STD) NMR, and SAR by NMR, have emerged as powerful methods for understanding the binding processes at both the molecular and atomic levels. Two types of NMR experimental approaches are generally used for studies of substrate−enzyme interactions. One focuses on the changes of NMR signals from the smaller substrate, such as trNOE and STD, whereas the other observes the chemical shift changes of the targeted protein (typically the amide $^{1}H-^{15}N$ single bond correlations, SAR by NMR) upon binding with its substrate. The trNOE NMR technique is particularly useful in the identification of a moderate, weak-binding ligand of a protein and determination of the bound conformation of the ligand

through quantitative analysis of the intramolecular trNOEs (*24*−*26*). In the present studies the 1D and trNOE NMR experiments have provided clear results for the identification of the interaction between U46619 and the engineered active PGIS. 3D structural determination of the PGIS-bound U46619, including the NOEs' changes from a strong negative to positive and the intramolecular trNOEs of the bound U46619, is important experimental evidence that supports the idea that PGH_2 must adopt a unique structure when bound to a COX-downstream synthase; in this case it is PGIS.

In the current studies, to control the spin diffusion which might affect the trNOEs resulting from the binding to the protein, we have used the following strategies: (1) Using less protein, since less protein appears to give less spin diffusion as identified by previous investigators (*27*). Since the bound ligand is very small, when a small amount of protein is used, a relatively long mixing time (300 ms) can be applied to the experiment to get the necessary intensity of NOESY. In other words, the spin diffusion effects of using a longer mixing time can be partially canceled by using a lower concentration of protein. (2) Using different mixing times for the NMR experiments. After comparison of the bound structures of U46619 obtained with the 150 and 300 ms mixing times, no significant differences were found, which indicated that little spin diffusion affects the experiments even when using a 300 ms mixing time. In fact, several experimental results have proven that the intermolecular spin diffusion is not a general problem for bound ligand determination in the designed trNOE experiments (*28*).

The D-ring propionate group in the crystal structure is not very well defined, but it is likely to point toward the distal pocket of the heme, a characteristic very distinct from that of other P450's (*13*). Our docking study indicated that the D-ring propionate group could form a hydrogen bond with the hydroxyl group on C-15 of U46619, which provides a possible explanation for its orientation. Our previous studies, which involve the use of a synthetic peptide, NMR, and mutagenesis techniques, have predicted that the L214 and P215 residues in the F/G loop are involved in the substrate docking (*23*, *28*, *29*). Furthermore, the current studies shown in Figure 8 confirmed that the L214 residue could form a part of the substrate binding pocket and P215 is located in the substrate access channel, which could be involved in regulating the substrate access to its active site.

The studies described above also provided important information for addressing the reaction mechanisms for the synthase. For example, one of the major conformational changes of U46619 bound to PGIS is the distance between C-6 and H2C, which directly relates to the reaction mechanism for the isomerization of PGH_2 to PGI_2. The distance between C-6 and H2C of U46619 changed from 4.62 to 3.99 Å (Figure 7) upon interaction with PGIS. A similar conformational change is expected in PGH_2 bound to PGIS. In this case, the change is favorable for the oxygen at C-9 to attack C-6 and isomerize PGH_2 to PGI_2, which is consistent with the proposed catalytic mechanism of PGIS from earlier studies (*11*). The second point is the hydrophobic tail between C-16 and C-20, which folded back and changed from a linear conformation to a hooklike conformation (Figure 8). The docking model of U46619 bound to PGIS clearly indicates that this hooklike structure from C-16 to C-20 is necessary for U46619 to fit into the relatively small substrate binding pocket of PGIS and interact with Trp282, which allows the substrate to sit in the pocket with a precise orientation (Figure 8). The fact that the replacement of Trp282 with a Phe residue could destroy the constraints that determine the specific orientation of U46619 as it moves into the active site (Figure 9) implies the importance of the Trp residue in the determination of the specific orientation of PGH_2 when binding to the PGIS active site during the biosynthesis of PGI_2. Phe was chosen for the Trp282 mutation because it has a side chain similar in size to that of Trp. However, it should be noted that this size may still not be large enough to generate the constraints which contact U46619 (Figure 9B), and therefore, it is possible for U46619 to become rotated to another undefined position. In addition, Phe was chosen because it has not been observed in other species in the corresponding residue of Trp282. This information has further allowed us to speculate that the bulky side chain of Trp (set in the substrate binding site) could be a unique configuration for the PGH_2 docking in the correct position that would cause it to be catalyzed into PGI_2, and not TXA_2.

To obtain a high-quality trNOE spectrum, it is crucial that the free U46619 and bound U46619 have a fast exchange rate, in which the signals of the PGIS-bound U44069 are quickly transferred to the free U46619 in solution and the line shape can still remain sharp. It is known that the K_d for the binding of U46619 to PGIS is in the lower micromolar range. This range of binding allows for high-quality trNOE spectra to be obtained. The method used in the present studies is particularly useful for studying the substrate−enzyme interactions for microsomal P450's, which have substrate binding properties similar to that of PGIS. However, one way to further increase the resolution of the trNOE experiments would be to use the deuterated protein.

PGH_2 is a common substrate shared by the COX-downstream synthases, including PGIS, TXAS, and PGE_2, PGD_2, and PGF_2 synthases. Understanding the molecular basis of how this common substrate could be converted into different prostanoids by their individual synthases has remained a challenge (*3*, *9*, *10*). By comparing the conformations of PGH_2 bound to the active sites of PGIS and TXAS (*14*) in solution, we can hypothesize that certain unique structural properties such as the nonconserved Trp282 in contact with PGH_2 and the shorter distance between the C-6 and C-9 positions of PGH_2 are involved in the isomerization of PGH_2 to PGI_2 by PGIS.

ACKNOWLEDGMENT

We thank Dr. Xiaolian Gao in the Chemistry Department and Dr. Youlin Xia in the KECK/IMD NMR Center of the University of Houston for access to the NMR facility and for providing valuable advice on taking the NMR spectra.

REFERENCES

1. Majerus, P. W. (1983) Arachidonate metabolism in vascular disorders, *J. Clin. Invest. 72*, 1521−1525.
2. Miller, D. K., Sadowski, S., Soderman, D. D., and Kuehl, F. A., Jr. (1985) Endothelial cell prostacyclin production induced by activated neutrophils, *J. Biol. Chem. 260*, 1006−1014
3. Smith, W. L. (1986) Prostaglandin biosynthesis and its compartmentation in vascular smooth muscle and endothelial cells, *Annu. Rev. Physiol. 48*, 251−262.

4. Picot, D., Loll, P. J., and Garavito, R. M. (1994) The X-ray crystal structure of the membrane protein prostaglandin H2 synthase-1, *Nature 367*, 243−249.
5. Kurumbail, R. G., Stevens, A. M., Gierse, J. K., McDonald, J. J., Stegeman, R. A., Pak, J. Y., Gildehaus, D., Miyashir, J. M., Penning, T. D., Seibert, K., Isakson, P. C., and Stallings, W. C. (1996) Structural basis for selective inhibition of cyclooxygenase-2 by anti-inflammatory agents, *Nature 384*, 644−648.
6. Ren, Y., Walker, C., Loose-Mitchell, D. S., Deng, J., Ruan, K. H., and Kulmacz, R. J. (1995) Topology of prostaglandin H synthase-1 in the endoplasmic reticulum membrane, *Arch. Biochem. Biophys. 323*, 205−214.
7. Needleman, P., Turk, J., Jackschik, B. A., Morrison, A. R., and Lefkowith, J. B. (1986) Arachidonic acid metabolism, *Annu. Rev. Biochem. 55*, 69−102.
8. Granstrom, E., Diczfalusy, U., Hamberg, M., Hansson, G., Malmsten, C., and Samuelson, B. (1982) in *Prostaglandins and the Cardiovascular System* (Oates, J. A., Ed.) pp 15−58, Raven Press, New York.
9. Ruan, K. H., Wang, L. H., Wu, K. K., and Kulmacz, R. J. (1993) Amino-terminal topology of thromboxane synthase in the endoplasmic reticulum, *J. Biol. Chem. 268*, 19483−19490.
10. Ruan, K. H., Li, P., Kulmacz, R. J., and Wu, K. K. (1994) Characterization of the structure and membrane interaction of NH2-terminal domain of thromboxane A2 synthase, *J. Biol. Chem. 269*, 20938−20942.
11. Hecker, M., and Ullrich, V. (1989) On the mechanism of prostacyclin and thromboxane A2 biosynthesis, *J. Biol. Chem. 264*, 141−150.
12. Ullrich, V., and Brugger, R. (1994) Prostacyclin and thromboxane synthase: new aspects of hemethiolate catalysis, *Angew Chem., Int. Ed. Engl. 33*, 1911−1919.
13. Chiang, C. W., Yeh, H. C., Wang, L. H., and Chan, N. L. (2006) Crystal structure of the human prostacyclin synthase, *J. Mol. Biol. 364*, 266−274.
14. Ruan, K. H., Wu, J., and Wang, L. H. (2005) Solution structure of a common substrate mimetic of cyclooxygenase-downstream synthases bound to an engineered thromboxane A2 synthase using a high-resolution NMR technique, *Arch. Biochem. Biophys. 444*,-165−173.
15. Yeh, H. C., Hsu, P. Y., Wang, J. S., Tsai, A. L., and Wang, L. H. (2005) Characterization of heme environment and mechanism of peroxide bond cleavage in human prostacyclin synthase, *Biochim. Biophys. Acta 1738*, 121−132.
16. Callihan, D., West, J., Kumar, S., Schweitzer, B. I., and Logan, T. M. (1996) Simple, distortion-free homonuclear spectra of peptides and nucleic acids in water using excitation sculpting, *J. Magn. Reson. B. 112*, 82−85.
17. Wüthrich, K. (1986) *NMR of Proteins and Nucleic Acids*, Wiley, New York.
18. Paulsen, M. D., and Ornstein, R. L. (1991) A 175-psec molecular dynamics simulation of camphor-bound cytochrome P-450cam, *Proteins 11*, 184−204.
19. Paulsen, M. D., and Ornstein, R. L. (1992) Predicting the product specificity and coupling of cytochrome P450cam, *J. Comput.-Aided Mol. Des. 6*, 449−460.
20. Shyue, S. K., Ruan, K. H., Wang, L. H., and Wu, K. K. (1997) Prostacyclin synthase active sites. Identification by molecular modeling-guided site-directed mutagenesis, *J. Biol. Chem. 272*, 3657−3662.
21. Landy, S. B., and Rao, B. D. N. (1989) Dynamical NOE in multiple-spin systems undergoing chemical exchange, *J. Magn. Reson. 81*, 371−377.
22. Lippens, R. M., Cerf, C., and Hallenga, K. (1992) Theory and experimental results of transfer-NOE experiments. 1. The influence of the off rate versus cross-relaxation rates, *J. Magn. Reson. 99*, 268−281.
23. Deng, H., Wu, J., So, S. P., and Ruan, K. H. (2003) Identification of the residues in the helix F/G loop important to catalytic function of membrane-bound prostacyclin synthase, *Biochemistry 42*, 5609−5617.
24. Leone, M., Freeze, H. H., Chan, C. S., and Pellecchia, M. (2006) The Nuclear Overhauser Effect in the lead identification process, *Curr. Drug Discovery Technol. 3*, 91−100.
25. Angulo, J., Rademacher, C., Biet, T., Benie, A. J., Blume, A., Peters, H., Palcic, M., Parra, F., and Peters, T. (2006) NMR analysis of carbohydrate-protein interactions, *Methods Enzymol. 416*, 12−30.
26. Megy, S., Bertho, G., Gharbi-Benarous, J., Baleux, F., Benarous, R., and Girault, J. P. (2006) STD and TRNOESY NMR studies for the epitope mapping of the phosphorylation motif of the oncogenic protein beta-catenin recognized by a selective monoclonal antibody, *FEBS Lett. 580*, 5411−5422.
27. Campbell, P. A, and Sykes, B. (1991) Theoretical evaluation of the two-dimensional transferred nuclear Overhauser effect, *J. Magn. Reson. 93*, 77−92.
28. Post, C. B. (2003) Exchange-transferred NOE spectroscopy and bound ligand structure determination, *Curr. Opin. Struct. Biol. 13*, 581−588.
29. Deng, H., Huang, A., So, S. P., Lin, Y. Z., and Ruan. K. H. (2002) Substrate access channel topology in membrane-bound prostacyclin synthase, *Biochem. J. 362*, 545−551.
30. Wang, L. H., Matijevic-Aleksic, N., Hsu, P. Y., Ruan, K. H., Wu, K. K., and Kulmacz, R. J. (1996) Identification of thromboxane A2 synthase active site residues by molecular modeling-guided site-directed mutagenesis, *J. Biol. Chem. 271*, 19970−19975.

BI701671Q